Unique properties of supramolecular biomaterials through nonequilibrium self-assembly

11

Raphael K. Grötsch, Job Boekhoven
Department of Chemistry and Institute for Advanced Study, Technical University of Munich, Garching, Germany

11.1 Introduction

In this chapter, we focus on nonequilibrium self-assembly of molecules into supramolecular assemblies. In nonequilibrium assemblies, there is a net exchange of energy and matter between the assembly and its environment. We further subdivide these assemblies in kinetically trapped assemblies, metastable assemblies, and dissipative nonequilibrium assemblies. In the first section, we will explain the subdivision in these classes and their relation with their free-energy landscapes. We will then detail each example with state-of-the-art man-made assemblies and highlight the unique material properties for each class of nonequilibrium assemblies, followed by examples of supramolecular biomaterials for each class. We will close this chapter with a perspective on where the field could benefit from a better understanding and especially better design rules for nonequilibrium assemblies.

11.2 The free energy landscapes of self-assembly

In supramolecular materials, molecules are assembled into molecular architectures with function [1]. The assembly process is driven by noncovalent, relatively weak, and thus reversible interactions between the molecules [2]. Self-assembly of molecules has been an active field of research, in part because the increasing understanding of the process has allowed to develop structures with entirely new properties. While most of the attention in the field has gone to supramolecular materials that are formed by self-assembly in equilibrium, recent attention has also focused on supramolecular materials that reside outside of equilibrium. In this section, we will discuss three types of assemblies based on their thermodynamic and kinetic properties and compare those in terms of their energy landscapes (Fig. 11.1).

Most of the attention in the field of supramolecular materials has gone to assemblies that are in equilibrium with their environment. Such assemblies can be observed when the noncovalent interactions between building blocks are relatively weak such

Self-Assembling Biomaterials. https://doi.org/10.1016/B978-0-08-102015-9.00012-5
Copyright © 2018 Elsevier Ltd. All rights reserved.

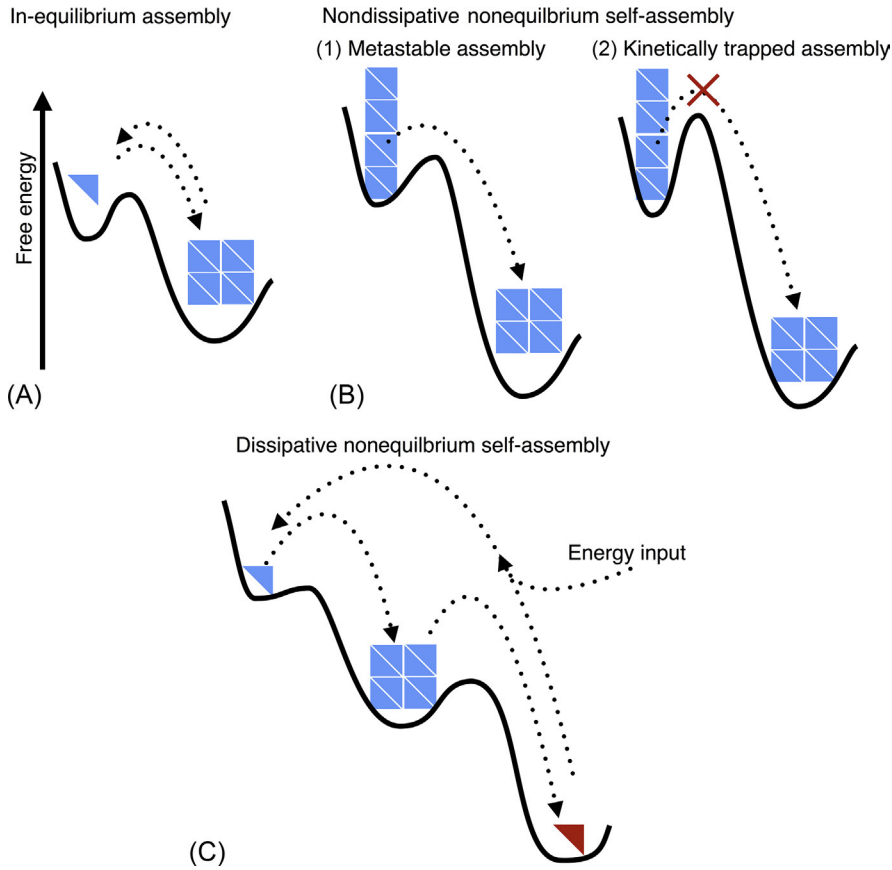

Fig. 11.1 Energy landscapes of self-assembly. Schematic representation of energy landscapes involved in the self-assembly of biomaterials. (A) In-equilibrium assemblies. (B) Out-of-equilibrium assemblies in a kinetic trap. (C) Dissipative nonequilibrium assemblies driven by chemical reaction networks.

that the thermal energy of the molecules allows relatively high exchange dynamics of nonassembled molecules with assembled ones. The rapid exchange with building blocks from the environment result in a system that can optimize its thermodynamically most favored state. Simply put, when a building block miss-assembles, the high exchange dynamics ensure rapid correction to an energetically more favorable state. The favored state corresponds to a state at the global minimum of the energy landscape [3]. In essence, the building blocks can reversibly exchange with the environment to find the most favorable state.

When the noncovalent interactions between building blocks are relatively strong, exchange of building blocks with the environment becomes slower. Consequently, the optimization to find the lowest state in the landscape is slower or sometimes even impossible. As the system is optimizing its configuration to find its thermodynamically most favored state, there is a net exchange of matter and energy between the assembly

and the rest of the system. The assembly is thus not in equilibrium with it environment. The process is referred to as nondissipative nonequilibrium self-assembly [4]. These nonequilibrium assemblies can be further divided into assemblies that do not exchange matter with their environment on any noticeable timescales and are thus "kinetically trapped" and assemblies that do exchange matter with their environment and slowly convert in their thermodynamically favored state, so-called metastable assemblies. In both cases of nonequilibrium self-assembly, the self-assembled state and thus its material properties are strongly dependent on the pathway of preparation as the self-assembled state is lacking the self-correcting mechanism that assemblies in equilibrium are endowed with. This pathway complexity can have great implications on the material properties of the self-assembled architectures [5,6].

A final type of self-assembly that we will discuss is dissipative nonequilibrium self-assembly [7]. In dissipative self-assembly, the self-assembling building blocks and their assemblies are thermodynamically unfavored. In fact, the building blocks constantly degrade to their thermodynamically more favored precursors, typically via a chemical reaction. In order to sustain the assemblies, a second chemical reaction has to constantly form the self-assembling building blocks from precursors. The ensemble results in building blocks that are constantly formed, while others are degraded. Although this mode of self-assembly might seem elaborate and complicated, it comes with unique material properties that are, in the context of supramolecular materials, vastly underexplored [8,9].

11.3 In-equilibrium self-assembly

When the noncovalent interactions between molecular building blocks are relatively weak, that is, comparable with thermal energies, a reversible ensemble is created in which the assembly can exchange building blocks with its environment. The reversibility is crucial for in-equilibrium self-assembly as it allows for a dynamic system that can try multiple modes of assemblies and self-correct to find the thermodynamically most favored state [10]. Most examples of man-made self-assembled structures are equilibrium assemblies. When assemblies are in equilibrium, we understand most of the processes at play. And because we understand, we can control and even design such materials [11–13]. In the past decades, the field of self-assembly and supramolecular materials has slowly evolved out of an era of serendipity into a time where design rules can be applied to develop materials built from the bottom up with nanometer precision. As a result, most supramolecular biomaterials will fit under this category [14,15].

In the context of biomaterials, a particularly successful and well-understood example of equilibrium assembly are the peptide amphiphiles (PAs) [16,17]. These molecules comprise three molecular domains that are important for their assembly. First, a hydrophobic domain, typically an aliphatic tail, drives molecules together by the hydrophobic effect. A second domain consists of amino acids that have a high propensity to form β-sheets. These directional interactions promote the formation of anisotropic fibers. A third domain comprises charged amino acids that ensure the fibers are water soluble [18].

A recent study on these PAs has demonstrated that these structures are in equilibrium with their environment, provided that the β-sheet domain undergoes relatively

weak interactions with neighboring PAs [19]. The elegant study used a PA that consisted of a 16-carbon alkyl tail connected to six alanine and three glutamic acid amino acids. The PAs were coassembled with very similar PAs labeled with either a green (cy3) or a red (cy5) fluorescent group. The resulting green and red fibers were mixed, and the exchange of building blocks between the two fibers was monitored by Förster resonance energy transfer (FRET). The FRET signal between cy3 and cy5 rapidly increased in the first hour and then steadily grew to a plateau value. The rate of increase in FRET signal was independent of the concentration of fibers, pointing to an exchange mechanism that is not diffusion limited. Based on these results, the authors hypothesize that the expulsion of single molecules or their reinsertion was the limiting step, similar to the exchange mechanism found for polymeric micelles [20]. The relatively rapid homogenization of the two mixed populations is a typical sign for in-equilibrium self-assembly.

Understanding the position of assemblers in the energy landscape facilitates the design of their corresponding supramolecular materials. For instance, recent work on very similar PAs has shown that a small alteration in their molecular design can make the difference between supramolecular fibers that can disrupt cell membranes and are thus toxic or supramolecular fibers that promote adhesion of cells [21]. The nontoxic PA consisted of a 16-carbon alkyl tail connected to three valine, three alanine, and three cationic lysine amino acids (PA 2). In contrast, the toxic PA consisted of a 16-carbon alkyl tail connected to three alanine, three glycine, and three cationic lysine amino acids (PA 1) (Fig. 11.2A and B). Both molecules formed seemingly similar cylindrical fibers with a diameter of 20 nm upon dispersion in water (Fig. 11.2C). However, as valine has here a higher propensity to form β-sheets compared with glycine, a difference in the ability to form strong hydrogen bonds was found. This difference was confirmed by FTIR measurements, and a strong Bragg reflection in the X-ray diffraction pattern showed crystalline hydrogen bonding of neighboring β-strands. Moreover, electron parametric resonance (EPR) spectroscopy revealed a decreased mobility of the molecules in the structures with stronger hydrogen bonding.

The subtle difference between the two PA molecules in their molecular structure evolved into the opposite behavior of cell proliferation. The lower β-sheet formation in PA 1 had a lower intermolecular cohesion. The structures were thus more dynamic, and the PAs likely interacted more with the lipid bilayer that induced cell death (Fig. 11.2D). Understanding the formation and the properties of the fibers from the molecular level up to the assembled structures opens up the possibility to design fibers that have the wanted characteristics.

11.4 Nondissipative nonequilibrium self-assembly: Metastable assemblies and kinetic traps

We demonstrated above that assemblies that are in equilibrium with their environment can exchange building blocks that endow them with a certain self-correction mechanism. Independent of the history of the system, including time since preparation or

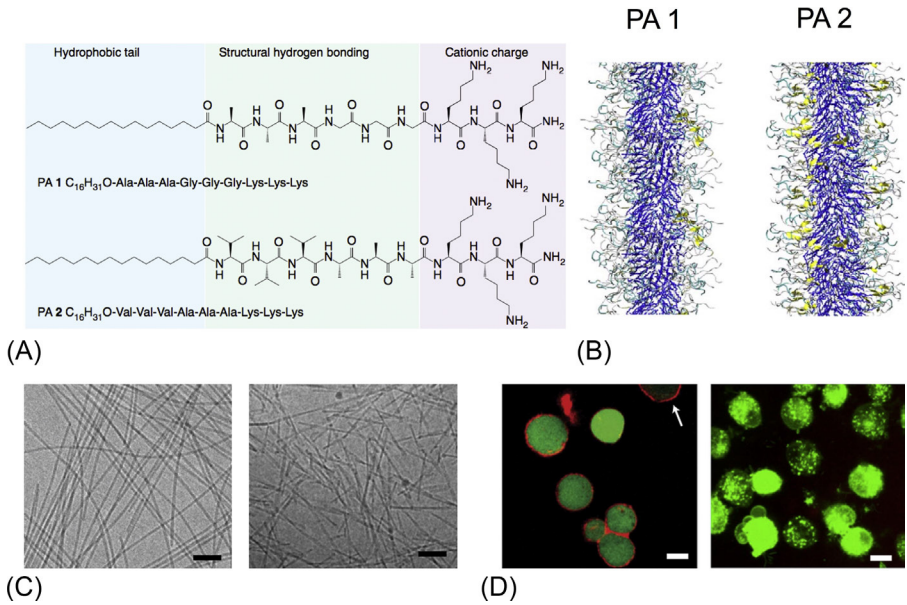

Fig. 11.2 (A) Chemical structures of PA 1 and PA 2 with equal alkyl tail length and equal number of lysine residues (cationic charge) but different propensity to form intermolecular hydrogen bonds. (B) Atomistic modeling reveals the different supramolecular interactions within the assemblies (yellow, cyan, gray, and blue indicate β-sheet hydrogen bonding, β-turn, random coil, and alkyl tail, respectively). (C) Cryo-TEM micrographs of representative assemblies in cell media. The scale bars corresponds to 100 nm. (D) Confocal micrographs of calcein stained cells settled on coatings of fluorescently labelled PA 1 (*left*) and PA 2 (*right*). Scale bars represent 10 μm.
Adapted from Newcomb CJ, Sur S, Ortony JH, Lee OS, Matson JB, et al. Cell death versus cell survival instructed by supramolecular cohesion of nanostructures. Nat Commun 2014;5:3321. Copyright 2014, Nature Publishing Group.

method of preparation, it will evolve to the same state at relatively high rates. When the noncovalent intermolecular interactions are strong, monomer exchange with the environment becomes slow or even unmeasurable [22]. In such cases, assemblies can be found in positions that are not the thermodynamically most favorable configuration and only slowly evolve to their favored configuration. When this is the case, we speak of nonequilibrium assemblies, as the assemblies are not in equilibrium with their surroundings. If the exchange is not observable on experimental timescales, the assemblies are kinetically trapped in the thermodynamically less favored states. If the exchange is observable but slow, the assemblies are metastable and slowly evolving to their favored state. In both cases, the systems lack the rapid self-correction mechanism, and the history of the assemblies plays a predominant role. The history of the assemblies is highly related to the method of sample preparations, which is why it is crucial to have a clear picture of these relations, especially in the context of supramolecular materials. In other words, when it comes to the development of supramolecular

materials that involve multiple, relatively strong interactions, not only the molecular design should be taken into consideration but also the preparative pathway. While this rule is well appreciated in the context of protein folding [23], in supramolecular materials, these relations have only recently been appreciated. In the following section, we will discuss examples of metastable assemblies and kinetically trapped assemblies and supramolecular materials.

11.4.1 Nondissipative nonequilibrium self-assembly: Metastable assemblies

A recent example by Meijer and coworkers [24] elegantly demonstrated the pathway complexity of metastable assemblies for the π-conjugated oligomer S-chiral oligo(*p*-phenylenevinylene) (SOPV, Fig. 11.3A). In methylcyclohexane (MCH) or other apolar solvents, these SOPVs self-assembled into helical structures. The authors used stopped-flow circular dichroism (CD) spectroscopy to analyze the pathway complexity and found the molecules self-assembled into either right- or left-handed helices depending on the preparative pathway (Fig. 11.3B). In earlier work, the left-handed helical aggregates were identified to be the thermodynamically most favored state [22].

Upon dispersion in apolar solvents, the molecules initially dimerized and subsequently formed disordered aggregates that developed into a nucleus. Once a critical number of building blocks in the nucleus was reached, the growth proceeded via further addition of dimers into a stack (Fig. 11.3C). While this mechanism is the same for both helices, the right-handed helix formed more rapidly than the left-handed one, resulting in an initial enrichment of the right-handed helix. Over time however, the metastable right-handed helices slowly disassembled to form the thermodynamically more favored left-handed helix. A kinetic model that was written to analyze protein fibrillization was used to further investigate the behavior of the assemblies. The model confirmed that the left-handed helix forms only under high monomer concentrations and low temperatures. With a SOPV concentration of 15 μM at 293 K, the CD signal at 466 nm showed for the first 100 s a positive signal indicating the formation of right-handed helixes. However, after the initial onset, the signal dropped to negative values, indicative of the right-handed stack, and stabilized after 3000 s. This example clearly demonstrates that the properties of the supramolecular material are dependent on the time since the preparation of the sample. Such knowledge is crucial when working with nonequilibrium supramolecular materials.

In the example above, the change is expressed in the chirality of the structures. Controlling the chirality is crucial for the functioning of supramolecular materials, and as such, a greater understanding of metastable nonequilibrium assemblies is important of the further development of the field of supramolecular (bio)materials. Moreover, such behavior not only is exclusive to SOPVs but also has been observed for other assemblers [25–28]. For example, the impressive work of Sugiyasu and coworkers investigated the self-assembly of a porphyrin molecule with alkyl chains into nanoparticles, nanofibers, or nanosheets [29]. Initially, a metastable product represented by nanoparticles formed. However, these nanoparticles transformed within 8 h to yield the thermodynamic more favored nanosheets.

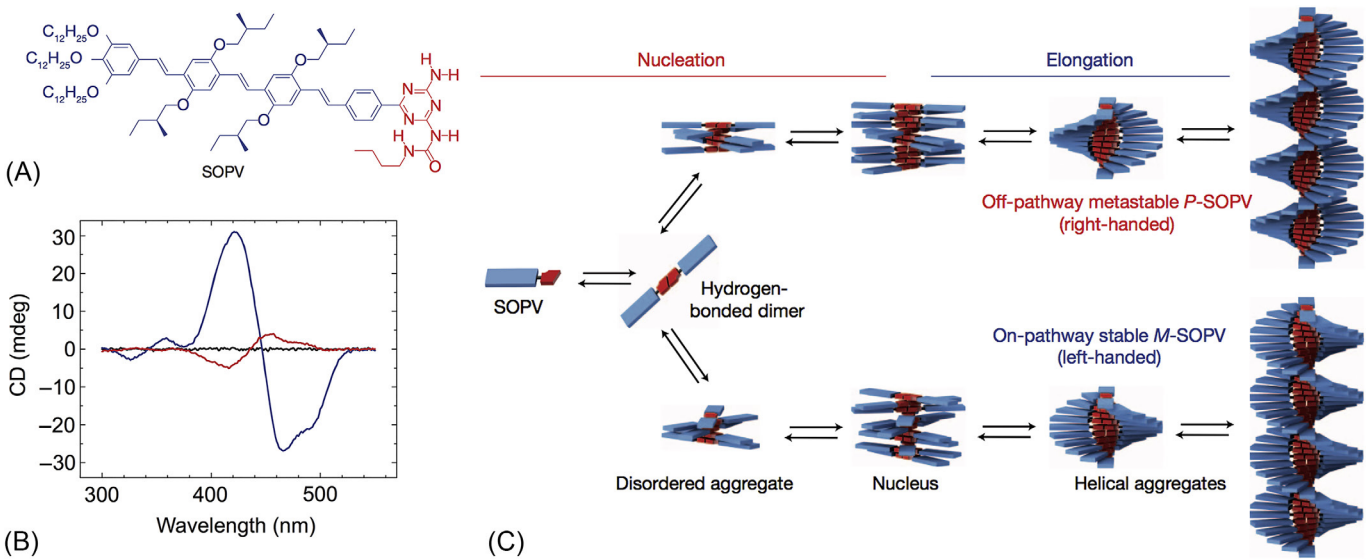

Fig. 11.3 (A) Molecular structure of monomeric SOPV. (B) CD spectra of SOPV in different energy and assembly states. *Black line*: monomeric state; *blue line*: thermodynamic state; *red line*: both M-SOPV and metastable P-SOPV in one sample. (C) Scheme showing two assembly pathways leading to two different helices. After the formation of a hydrogen bonded dimer and the formation of a nucleus, the assemblies continues to form helices. This is achieved by a nucleation elongation mechanism in apolar solvents. The right-handed (P) helix forms quickly but is less stable than the left hand (M) helix.
Adapted from Korevaar PA, de Greef TF, Meijer EW. Pathway complexity in π-conjugated materials. Chem Mater 2013;26:576–86.
Copyright 2012, Nature Publishing Group.

11.4.2 Nondissipative nonequilibrium self-assembly: Kinetic traps

In the examples above, metastable supramolecular assemblies relaxed over time to their thermodynamically favored state. In cases where such relaxation is unnoticeable, we speak of kinetically trapped states. In this class of nonequilibrium assembly, the structure is not in the thermodynamically most favored state, and the system does not have sufficient energy to overcome the barrier toward that state [30].

An example of assemblies that are kinetically trapped has been described by Ulijn and coworkers. They used peptides with aromatic groups that could enzymatically be converted into building blocks that assemble into fibers. The fibers entrapped their solvent resulting in the formation of hydrogels [31]. The aromatic peptide consisted of a dipeptide protected on the *N*-terminus with *N*-(fluorenyl-9-methoxycarbonyl) (Fmoc) group and on the C-terminus with a methyl ester (Fig. 11.4A). The methyl ester at the C-terminus of the dipeptide was hydrolyzed to the acid by subtilisin, a hydrolytic enzyme. The difference in molecular structure between the ester and acid was sufficient to induce a morphological transition from a solution state into fibers that entangled and formed a hydrogel (Fig. 11.4B). The aromatic dipeptides were incubated with different concentrations of enzyme for an hour at 55°C, after which the samples were cooled to room temperature. Using HPLC analysis, the authors could conclude that for each concentration of enzyme, full conversion to the carboxylic acid was reached. Moreover, for each concentration of enzyme, the sample had transformed into a hydrogel. However, the strength of the gel was not similar between samples. In fact, the higher the enzyme concentration, the higher the melting point of the gel (Fig. 11.4C). Fourier transformed infrared spectroscopy (FTIR) studies combined with CD spectroscopy confirmed the β-sheet formation between the peptides, while fluorescence emission spectra showed π-π stacking of the Fmoc groups. However, also here, the authors found

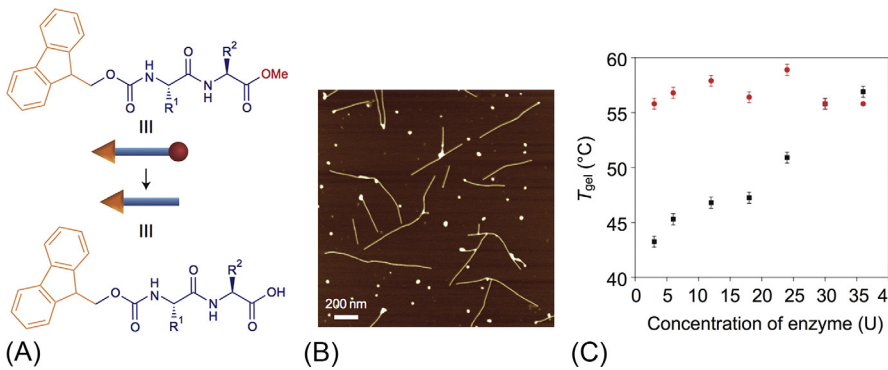

Fig. 11.4 (A) Fmoc-dipeptide methyl esters before and after the Subtilisin catalyzed hydrolysis to the corresponding acids. (B) AFM images showing the beginning of the agglomeration of fibers and clusters. (C) Diagram showing the melting temperature (T_{gel}) of gels. Black markers indicate the T_{gel} of gels with Subtilisin catalysis. Red markers specify the T_{gel} of gels after a heating cooling cycle.
Adapted from Hirst AR, Roy S, Arora M, Das AK, Hodson N, et al. Biocatalytic induction of supramolecular order. Nat Chem 2010;2:1089–94. Copyright 2010, Nature Publishing Group.

that the higher the enzyme concentration, the greater the signal for β-sheet formation. These observations are surprising, since each sample contains the exact same amount of aromatic dipeptide building blocks, under the exact same conditions (pH, temperature, and buffer). The only difference between the samples is a difference in concentration enzyme and thus a difference in rate of formation of the molecular building blocks for the fibers. Such differences in material properties depending on the preparative pathway (fast formation vs. slow formation) are a typical feature of kinetically trapped states. Indeed, the authors showed that the effect was a result of kinetic effects by annealing the samples to induce disassembly. The gels were reformed after gently cooling down these solutions. For these samples, the CD signals after a heating-cooling cycle of the samples with different catalyst concentrations were identical.

From the above example, it is clear that for supramolecular materials in which noncovalent interactions are relatively strong, the properties can depend on the preparative pathway as molecules can remain locked in kinetic traps. A greater understanding of such trapping mechanisms allows the user to tune their material properties simply by changing the preparative pathway and making use of the free-energy landscape. Studies by other groups have shown that this behavior not only is limited to enzymatic conversion of precursors but also can be induced by organocatalytic conversion of well-soluble precursors into hydrogel-forming assemblers [32]. The authors found, in line with the example above, that an increase rate of product formation results in an increased strength of the gels.

A recent study found that also the formation of fibers by PAs can be strongly dependent on the preparative pathway [32a]. This result might sound counterintuitive as we mentioned in Section 11.2 PA fibers that were in-equilibrium structures. We have to point out that this difference has to do with the noncovalent interactions between the PAs. The main difference between the two PAs is their ability to form β-sheets. While the PAs mentioned above with six alanine amino acids formed relatively weak β-sheets, the PAs that can be kinetically trapped into fibers comprise three valine and three alanine amino acids. Valine is known to have a higher propensity to form β-sheets compared with alanine [33]. The balance between forces that drive self-assembly can change the behavior of otherwise relatively similar molecules. The PA used in this study consisted of a 16-carbon chain, followed by three valine, three alanine, and three lysine amino acids. After the dissolution of the PA in water, preparation of the different supramolecular materials was achieved in two steps: annealing (heating to 80°C and gently cooling to room temperature) and dilution. It is important to note that annealing typically gives molecules sufficient energy to navigate the energy landscape and position themselves in the thermodynamically most favored configuration. Dilution on the other hand changes the environment of the assemblies and can thus bring the assemblies from one energy landscape to another.

The authors showed that freshly dissolved PA at a relatively high concentration (4.4 mM) was characterized by short fibers. These short fibers represented a metastable state in the energy landscape and slowly grew to long fibers driven by β-sheet formation as evidenced by cryo-TEM and CD spectroscopy. The long fibers were thus the thermodynamically favored state, and the transition to this state could be accelerated by an annealing step. When the fibers were diluted to a relatively low concentration (0.44 mM), the ionic repulsion between the lysine groups disfavored the

formation of β-sheets. As these β-sheets were the driving force for fiber elongation, the thermodynamically favored states under these conditions were short fibers as evidenced by cryo-TEM. The authors confirmed this by first diluting the metastable fibers at 4.4 to a concentration of 0.44 mM and then annealing the sample. This pathway resulted in the short thermodynamically favored fibers. In contrast, when the exact same sample was first annealed at a high concentration, giving long fibers, and then diluted to 0.44 mM, the long fibers were still found. The kinetically trapped long fibers were stable for months. In essence, the molecules in the long fibers did not have sufficient energy to disassemble and form the thermodynamically favored short fibers. Only upon reannealing the samples were the short fibers found (Fig. 11.5A).

The finding implies that two different morphologies can be found, for the exact same molecule under the exact same conditions. The only difference between the two samples is their history. Unsurprisingly, the difference in supramolecular structure resulted in different material properties. For instance, when immobilized on a surface, the interaction between cells and fibers was different. Fibroblast cells on surfaces that comprise the short fibers were unable to sufficiently adhere and remained relatively round (Fig. 11.5B). In contrast, the same cells on surfaces of the long fibers were able to adhere and elongate. Cells on the latter surface also survived for longer times. Using atomic force microscopy (AFM) studies, the authors found that the surface comprising long fibers was drastically better at sustaining pulling force compared with the surface of short fibers. It is thus hypothesized that the short fibers are not able to sustain the forces exerted by the fibroblasts, while the long fibers are. To further confirm the difference in material properties, the authors exposed cells to the fibers in solutions. It was found that the short fibers were significantly more toxic compared to the long fibers (Fig. 11.5C). The mechanism for the latter observation remains unclear, but the authors hypothesize that the increased number of endcaps on short fibers compared with long fibers might increase the ability of fibers to lethally penetrate the cells.

11.5 Dissipative nonequilibrium assembly

In dissipative nonequilibrium self-assembly, both the building blocks and its assemblies are thermodynamically unfavored. In fact, the thermodynamically favored state is a precursor state that does not assemble at all [9]. Only by the consumption of an external source of energy can the precursor be "pushed" out of equilibrium into a building block state that can assemble. Since the assemblies are not thermodynamically favored, they disassemble and revert to the precursor state. The energy source can be provided by means of chemical reactions. In the first reaction, the precursor is converted into the building block that can then assemble. As the activation pushes the precursor higher in the energy landscape, it is not a spontaneous reaction, but it is driven by the consumption of a sacrificial high-energy species. This high-energy species can be a photon in photochemical activation reaction or a small molecule such as the ubiquitous adenosine triphosphate (ATP) or guanosine triphosphate (GTP) in biology [34]. Upon activation, the building block can self-assemble. Crucially, the building

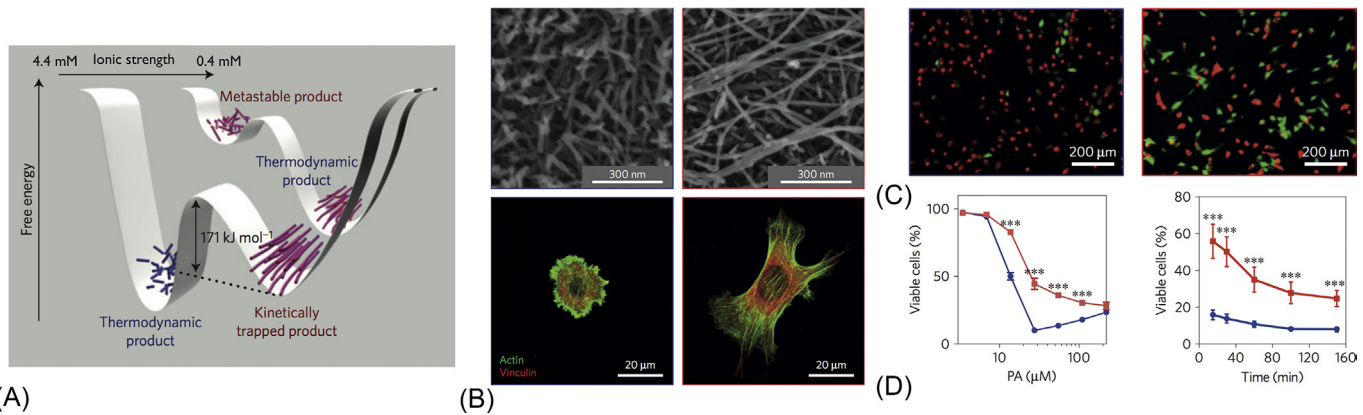

Fig. 11.5 (A) Illustration of the free energy landscapes of PA assemblies with the free energy on the *y*-axis and the ionic strength from 4.4 to 0.4 mM on the *x*-axis. The ionic strength influences the β-sheet formation, so that low concentration leads to short fibers in a metastable state and long fibers in a thermodynamic state. For a high concentration of 4.4 mM the stable product is short fibers and a kinetically trapped long fiber product appears with an energy barrier of 171 kJ mol^{-1}. (B) SEM showing the same PA with short or long fibers. Cells observed with immunofluorescent staining showing relatively rounds cells as a sign of bad attachment to the short fibers and a spread cell as a sign for successful attachment to surface of long fibers. (C) C2C12 premyoblasts in cell media with short (*left*) and long (*right*) PA fibers after 3 h. Green indicates living cells and red shows dead cells (*upper left and right*). (D) Viable cells in relation to PA concentration after 3 h (*lower left*). Viable cells with 110 μM PA monitored over time (*lower right*).

Adapted from Tantakitti F, Boekhoven J, Wang X, Kazantsev RV, Yu T, Li J, et al. Energy landscapes and functions of supramolecular systems. Nat Mater 2016;15(4):469–76. Copyright 2016, Nature Publishing Group.

block spontaneously deactivates into the thermodynamically favored precursor. After deactivation, the precursor can undergo another cycle.

A pioneering example of molecular dissipative self-assembly driven by chemical reaction networks has been described by van Esch and coworkers [35]. That work used *N*,*N*′-dibenzoyl-L-cystine (DBC), a dicarboxylate that was well soluble in water, as a precursor (Fig. 11.6A and B) [36]. It was found that the carboxylates of DBC could be methylated into the corresponding methyl ester by methylating agents such as methyl iodide (MeI) and dimethyl sulfate (DMS) to yield DBC-OMe_2. For instance, the authors described that addition of a batch of 100 mM of MeI to 100 mM DBC resulted in the formation of the mono- and diesters of it corresponding dicarboxylate. Crucially, in the aqueous environment, the ester was an unstable molecule, and it slowly hydrolyzed back to the original precursor (DBC) state. After about 100 h, a maximum in ester concentrations was found, whereas after 350 h, all ester had been hydrolyzed, and thus, all DBC had been recovered. At 400 h, a second batch of methyl iodide was added and the cycle repeated.

Lacking the two anionic dicarboxylates, the diester building block was much less soluble than its corresponding precursor. In fact, the ester was found to self-assemble into fibers by electron microscopy studies. By means of dynamic light scattering, the turbidity of the samples was measured in response to the addition of the fuel. The signal transiently increased with a similar lifetime as the esters, pointing to the formation of large assemblies when the esters are present. Finally, electron microscopy revealed the presence of fibers in samples that had been exposed to the methyl iodide (Fig. 11.6C and D).

Coupling the assembly of building blocks to energy dissipating chemical reaction networks is cumbersome and elaborate, but it comes with unique properties that remain largely unexplored. The authors showed in follow-up work [37] that the lifetime of the corresponding fibrillar materials can be controlled by kinetic parameters, such as the initial amount of methylating agent added or the pH of the system, resulting in gels that are present for hours or weeks. Such temporal control over material properties opens the door to unique supramolecular materials that disintegrate at predefined times. Moreover, it was demonstrated that the corresponding materials were self-healing, provided that the system contained sufficient amounts of methylating agent.

Clearly, the use of toxic methylating agents to drive the assembly makes them unsuitable as applicable biomaterials. However, more recent work has shown that dissipative nonequilibrium self-assembly is not limited to dicarboxylate ester conversion. For instance, Ulijn and coworkers showed that transient and dynamic fiber formation could be induced by a chemical reaction network that uses α-chymotrypsin to condense a well-soluble amine with a methyl ester into an amide that self-assembled into hydrogel-forming fibers [38]. The authors chose the conditions such that the enzyme also hydrolyzes the amide product to the original amine and a carboxylate waste product. In this system, the cycle time was tunable in the range of 200–1000 min with the amount of enzyme. As a result, the authors could develop transient hydrogels with lifetimes in the order of roughly 100–600 min.

In recent work, our group introduced a chemical reaction network based on the condensation of a dicarboxylate into its corresponding anhydride at the expense of a

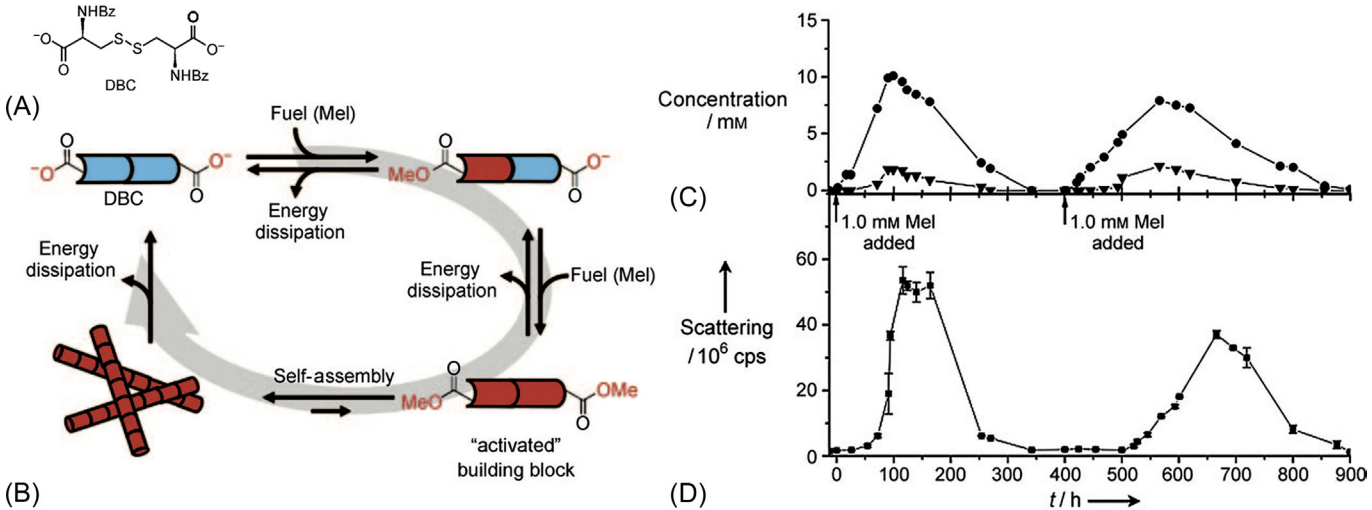

Fig. 11.6 (A) Molecular structure of *N*,*N*′-dibenzoyl-L-cystine (DBC) is the precursor in this study. (B) Chemical reaction network that drives the dissipative self-assembly formation of fibers. The precursor (DBC, *blue*) can react twice with high-energy methylating agent MeI resulting in the formation of the activated building block (diester, *red*). The activated building block self-assembles into fibers but is intrinsically unstable and slowly hydrolyzes back to the original DBC precursor. (C) Concentration profiles of mono- *(circle)* and diester *(triangle)* and (D) scattering profiles in response to an addition of 1 mmol of MeI to 100 mM DBC. After 400 h, a second 1 mmol batch is added in order to start a second cycle.

Adapted from Boekhoven J, Brizard AM, Kowlgi KN, Koper GJ, Eelkema R, et al. Dissipative self-assembly of a molecular gelator by using a chemical fuel. Angew Chem Int Ed Eng 2010;49:4825–8. Copyright 2010, John Wiley & Sons.

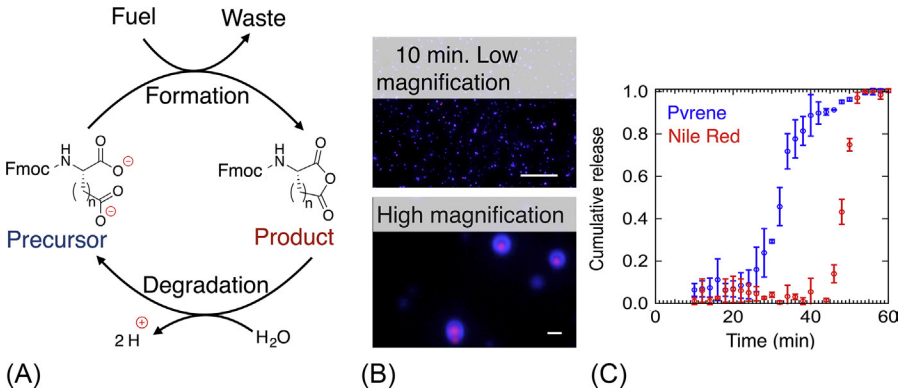

Fig. 11.7 (A) Chemical reaction network that drives the dissipative nonequilibrium self-assembly formation of fibers. The precursor can react with high-energy carbodiimide fuels resulting in the formation of the activated anhydride product. The activated building block is intrinsically unstable and rapidly hydrolyzes back to the original precursor. (B) Fluorescence microscopy of the transient colloids formed by Fmoc-E in response to EDC as a fuel. EDC was added to 10 mM Fmoc-E with 2.5 μM Nile red *(red)*. After 5 min, 25 μM pyrene *(blue)* was added. The sequential addition of the dyes resulted in incorporation of the Nile red in the core of the particles, while the pyrene was mostly found in the outer layers. (C) Release profiles of pyrene and Nile red of the particles described in (B). Adapted from Tena-Solsona M, et al. Non-equilibrium dissipative supramolecular materials with a tunable lifetime. Nat Commun 2017;8:15895. https://doi.org/10.1038/ncomms15895. Copyright 2017, Nature Publishing Group.

high-energy carbodiimide fuel [39]. While the dicarboxylate precursor had two negative charges, the anhydride product was uncharged (Fig. 11.7A). This hydrophobization was used to induce the self-assembly of the product. In the aqueous environment, the anhydride product was extremely labile and rapidly reacted back to the original precursor. For instance, while the Fmoc-glutamic acid precursor was well soluble, addition of 1-ethyl-3-(3-dimethylaminopropyl)carbodiimide (EDC) as a source of carbodiimide converted part of the acid into the anhydride that in turn self-assembled in colloids. The lifetime of the colloids could be tuned by the amount of EDC from minutes to hours. Moreover, the colloids could be loaded with various hydrophobic molecules in a sequential manner, resulting in particles with several layers of hydrophobic molecules (Fig. 11.7B). As the particles degraded, these hydrophobic molecules were released in a sequential manner, opening the door to drug delivery vehicles that can release hydrophobic agents in a sequential manner at predefined times (Fig. 11.7C).

11.6 Conclusion and future trends

In this chapter, we have illustrated the differences between in and out of equilibrium self-assembly. Because assemblies in equilibrium assemblies do not change over time, their material properties are constant and independent of history. In contrast, the properties of nondissipative nonequilibrium materials, which include metastable and

kinetically trapped assemblies, depend highly on their preparative pathway. Finally, in dissipative nonequilibrium self-assembly, the formation of materials is coupled to chemical reaction networks that result in materials that are dynamic and of which the lifetime can be tuned by kinetics. In the context of biomaterials, the latter has been ill-explored.

References

[1] Amabilino DB, Smith DK, Steed JW. Supramolecular materials. Chem Soc Rev 2017;46:2404.
[2] Whitesides GM, Grzybowski B. Self-assembly at all scales. Science 2002;295:2418–21.
[3] Whitesides GM, Boncheva M. Beyond molecules: self-assembly of mesoscopic and macroscopic components. Proc Natl Acad Sci U S A 2002;99:4769–74.
[4] Sorrenti A, Leira-Iglesias J, Markvoort AJ, de Greef TF, Hermans TM. Non-equilibrium supramolecular polymerization. Chem Soc Rev 2017;46:5476–90.
[5] Ogi S, Fukui T, Jue ML, Takeuchi M, Sugiyasu K. Kinetic control over pathway complexity in supramolecular polymerization through modulating the energy landscape by rational molecular design. Angew Chem Int Ed Eng 2014;53:14363–7.
[6] Fukui T, Kawai S, Fujinuma S, Matsushita Y, et al. Control over differentiation of a metastable supramolecular assembly in one and two dimensions. Nat Chem 2016;9:493–9.
[7] Grzybowski BA, Wilmer CE, Kim J, Browne KP, Bishop KJM. Self-assembly: from crystals to cells. Soft Matter 2009;5:1110–28.
[8] Fialkowski M, Bishop KJ, Klajn R, Smoukov SK, Campbell CJ, et al. Principles and implementations of dissipative (dynamic) self-assembly. J Phys Chem B 2006;110:2482–96.
[9] van Rossum SAP, Tena-Solsona M, van Esch JH, Eelkema R, Boekhoven J. Dissipative out-of-equilibrium assembly of man-made supramolecular materials. Chem Soc Rev 2017;46:5519–35.
[10] Whitesides GM, Boncheva M. Beyond molecules: self-assembly of mesoscopic and macroscopic components. Proc Natl Acad Sci U S A 2002;99:4769–74.
[11] Ulijn RV, Smith AM. Designing peptide based nanomaterials. Chem Soc Rev 2008;37:664–75.
[12] Van Esch JH. We can design molecular gelators, but do we understand them? Langmuir 2009;25:8392–4.
[13] Cui H, Webber MJ, Stupp SI. Self-assembly of peptide amphiphiles: from molecules to nanostructures to biomaterials. Biopolymers 2010;94:1–18.
[14] Webber MJ, Appel EA, Meijer EW, Langer R. Supramolecular biomaterials. Nat Mater 2016;15:13–26.
[15] Boekhoven J, Stupp SI. 25th anniversary article: supramolecular materials for regenerative medicine. Adv Mater 2014;26:1642–59.
[16] Hartgerink JD, Beniash E, Stupp SI. Self-assembly and mineralization of peptide-amphiphile nanofibers. Science 2001;294:1684–8.
[17] Hartgerink JD, Beniash E, Stupp SI. Peptide-amphiphile nanofibers: a versatile scaffold for the preparation of self-assembling materials. Proc Natl Acad Sci U S A 2002;99:5133–8.
[18] Cui H, Webber MJ, Stupp SI. Self-assembly of peptide amphiphiles: from molecules to nanostructures to biomaterials. Biopolymers 2010;94:1–18.
[19] Da Silva RM, Van Der Zwaag D, Albertazzi L, Lee SS, Meijer EW, et al. Super-resolution microscopy reveals structural diversity in molecular exchange among peptide amphiphile nanofibres. Nat Commun 2016;7:11561.

[20] Lund R, Willner L, Richter D, Dormidontova EE. Equilibrium chain exchange kinetics of diblock copolymer micelles: tuning and logarithmic relaxation. Macromolecules 2006;39:4566–75.
[21] Newcomb CJ, Sur S, Ortony JH, Lee OS, Matson JB, et al. Cell death versus cell survival instructed by supramolecular cohesion of nanostructures. Nat Commun 2014;5:3321.
[22] Jonkheijm P, Van Der Schoot P, Schenning AP, Meijer EW. Probing the solvent-assisted nucleation pathway in chemical self-assembly. Science 2006;313:80–3.
[23] Chiti F, Dobson CM. Protein misfolding, functional amyloid, and human disease. Annu Rev Biochem 2006;75:333–66.
[24] Korevaar PA, George SJ, Markvoort AJ, Smulders MM, Hilbers PA, et al. Pathway complexity in supramolecular polymerization. Nature 2012;481:492–6.
[25] Sorrenti A, Leira-Iglesias J, Markvoort AJ, De Greef TF, Hermans TM. Non-equilibrium supramolecular polymerization. Chem Soc Rev 2017;46:5476–90.
[26] Korevaar PA, de Greef TF, Meijer EW. Pathway complexity in π-conjugated materials. Chem Mater 2013;26:576–86.
[27] Haedler AT, Meskers SC, Zha RH, Kivala M, et al. Pathway complexity in the enantioselective self-assembly of functional carbonyl-bridged triarylamine trisamides. J Am Chem Soc 2016;138:10539–45.
[28] Adelizzi B, Filot IAW, Palmans ARA, Meijer EW. Unravelling the pathway complexity in conformationally flexible N-centered triarylamine trisamides. Chemistry 2017;23:6103–10.
[29] Fukui T, Kawai S, Fujinuma S, Matsushita Y, Yasuda T, et al. Control over differentiation of a metastable supramolecular assembly in one and two dimensions. Nat Chem 2017;9:493–9.
[30] Yan Y, Huang J, Tang BZ. Kinetic trapping—a strategy for directing the self-assembly of unique functional nanostructures. Chem Commun (Camb) 2016;52:11870–84.
[31] Hirst AR, Roy S, Arora M, Das AK, Hodson N, et al. Biocatalytic induction of supramolecular order. Nat Chem 2010;2:1089–94.
[32] Boekhoven J, Poolman JM, Maity C, Li F, Van Der Mee L, et al. Catalytic control over supramolecular gel formation. Nat Chem 2013;5:433–7.
[32a] Tantakitti F, Boekhoven J, Wang X, Kazantsev RV, Yu T, Li J, et al. Energy landscapes and functions of supramolecular systems. Nat Mater 2016;15(4):469–76.
[33] Levitt M. Conformational preferences of amino acids in globular proteins. Biochemistry 1978;17:4277–85.
[34] Kirschner M, Mitchison T. Beyond self-assembly: from microtubules to morphogenesis. Cell 1986;45:329–42.
[35] Boekhoven J, Brizard AM, Kowlgi KN, Koper GJ, Eelkema R, et al. Dissipative self-assembly of a molecular gelator by using a chemical fuel. Angew Chem Int Ed Eng 2010;49:4825–8.
[36] Menger FM, Caran KL. Anatomy of a gel Amino acid derivatives that rigidify water at submillimolar concentrations. J Am Chem Soc 2000;122:11679–91.
[37] Boekhoven J, Hendriksen WE, Koper GJ, Eelkema R, Van Esch JH. Transient assembly of active materials fueled by a chemical reaction. Science 2015;349:1075–9.
[38] Pappas CG, Sasselli IR, Ulijn RV. Biocatalytic pathway selection in transient tripeptide nanostructures. Angew Chem Int Ed Eng 2015;54:8119–23.
[39] Tena-Solsona M, et al. Non-equilibrium dissipative supramolecular materials with a tunable lifetime. Nat Commun 2017;8:15895. https://doi.org/10.1038/ncomms15895.